Rotational temperature profiles of shock waves in diatomic gases

By A. K. MACPHERSON

Department of Mechanical Engineering, University of Manitoba,
Winnipeg 19, Canada†

The variation of the translational temperature, rotational temperature, and density through shock waves in oxygen and nitrogen was studied using classical laws of mechanics and a Monte Carlo scheme. The collision dynamics were calculated using an intermolecular potential by Parker with both a two-dimensional approximation and the full three-dimensional calculations. The rotational velocity frequency distributions were also calculated. The average number of collisions a molecule will experience at various stages passing through a shock wave were found and plotted with the temperature and density profiles. The nitrogen results were compared with experimental results and good agreement was found. This also provided a method for giving a first approximation to the three-dimensional intermolecular potential.

Introduction

A number of authors have investigated theoretically relaxation processes in gases. These have included both classical treatments such as Taxman (1958) or Curtiss (1956) and quantum mechanical treatments such as Wang Chang, Uhlenbeck & de Boer (1964, p. 253). The resultant expressions have been solved for various idealized molecular models, some of which are listed in Lordi & Mates (1970). The assumptions concerning the idealized models often restricted the ability of the solution to be compared with experiment. Parker (1959) used a rather convincing molecular model which consisted of an attractive potential between the geometric centres of the molecules and two repulsive centres located along the internuclear axes of each molecule. A solution was obtained by assuming that the axes of rotation were perpendicular to the collision plane throughout the collision (two-dimensional calculation) and then using series expansions for the variables in the Lagrangian. One of the molecular potential constants, the distance between the repulsive centres of the molecule, was chosen by fitting the solution Parker obtained for vibrational relaxation to experimental results. An extension of Parker's work was performed for rotational relaxation by Lordi & Mates (1970). Here the equations of motion were extended to the full three-dimensional system, removing the approximation by Parker above,

† Present address: Department of Mechanical Engineering and Mechanics, Lehigh University, Bethlehem, Pennsylvania 18015.

and using a Monte Carlo method together with the work by Wang Chang, Uhlenbeck & Taxman (1961) to calculate transport properties. Using the same molecular potential as Parker (1959) it was found that the three-dimensional calculations did not give as good results as with the two-dimensional approximation. This was ascribed to the selection of the internuclear repulsive force distance by matching Parker's results to experiment. A larger value of this constant was suggested by Lordi & Mates (1970). All these calculations have assumed that translational temperature equilibrium has been achieved before the calculations start and that density is constant throughout the calculations.

On the other hand a theoretical study has been conducted (Talbot & Scala 1961, p. 603), with a view to studying the rotational relaxation through shock waves. This has differed from the above calculations in that the translational temperature is varying during the initial period of relaxation and that the density varies throughout the relaxation period. This study used modified Navier–Stokes equations and when the results were compared with the experimental results of Robben & Talbot (1966 b) it was found that the rotational collision number was $Z_R = 5$. As pointed out by Robben & Talbot (1966 b), the diffusion of rotational energy was neglected, which it is suggested may be important in certain regions of the shock wave.

One of the first attempts to measure the rotational relaxation through shock waves was by Muntz (1962) who pioneered the development of an electron beam fluorescence technique. This technique was later used by Robben & Talbot (1966 b) in a nitrogen low-density wind tunnel using free jet expansions from sonic orifices. It was found that the shock-wave rotational temperature profile appeared to separate from the shock density profile with increasing Mach number and move towards the translational temperature profile. It was not possible to measure the translational temperature profile; although it was found that the maximum slope shock-wave thickness was only about half of that previously measured using another technique by Camac (1966, p. 240). Using a similar free jet tunnel and an electron beam technique, Marrone (1967) conducted further experiments upon shock profiles in nitrogen. It was found that shock-wave thicknesses approximately twice that found by Robben & Talbot were obtained. The present work attempts to calculate the profiles of translational temperature, rotational temperature and density through shock waves in nitrogen and in oxygen, using a Monte Carlo technique to monitor the diffusional transfer of energy and the work by Lordi & Mates (1970) to calculate the collisional transfer of energy. Both the two-dimensional and three-dimensional calculations of collisional transfer of energy are used and compared. The nitrogen results are then compared with experiment. Unfortunately, the free jet expansions gave very low temperatures $\simeq 10\,°K$ for Mach 12·9 shock waves. The temperature upstream of the shock wave is in a region where the viscosity is not well defined. Thus the mean free path is difficult to calculate and comparison with the present results is a little difficult. It was found that the shock-wave thicknesses calculated were about twice that obtained by Talbot and thus lay close to those by Marrone (1967).

Monte Carlo technique

This technique consists of two aspects, a general accounting scheme which monitors the diffusional transfer of energy and a second aspect where the details of the collisional transfer of energy are calculated. The general scheme has been described previously (Macpherson 1969), so only an outline will be given here. The author will supply on request detail of the methodology to enable the interested reader to reconstruct the technique. Consider a gas dynamic system which is bounded by a wall at one end and a piston at the other. The volume is divided into K comparatively small subsystems or cells typically 1.5λ wide where λ is the mean free path. If the number density of the gas is n we will represent the gas on a computer by N particles per cell. The NK particles of the whole system are assigned random positions throughout the volume and have both translational and rotational velocities chosen from the appropriate Maxwellian distributions. During a short interval of time ΔT_m, the particles are assumed to remain within the initial cell and to transfer energy by collisions. Let σ_{ij} be the collision cross-section for two particles i and j which have velocities V_i and V_j in a given cell k. As shown in Macpherson (1969), using the theory by Denisik, Malama, Polak & Rezanov (1967), the time of flight t_i of the ith particle before a collision is

$$t_i = \frac{-\ln \xi_i N}{n \Sigma |V_i - V_j| \sigma_{ij}},$$

where ξ_i is a random number between 0 and 1.0. Thus the first particle in the subsystem k to collide is chosen as the one with minimum t_i. The colliding partner j is chosen as described in Macpherson (1969), new velocities are calculated as described below and time $\Delta T_i = 2t_i$ is considered to have elapsed. The procedure is repeated until $\Sigma \Delta T_i > \Delta T_m$ for all K cells. The particles and piston are then moved with their current velocities for time ΔT_m.

Consider now the collisional transfer of energy. The collisional dynamics used are as proposed by Lordi & Mates (1970). Each molecule of mass $2m$ and moment of inertia I in the colliding pair has two repulsive force centres located at a distance d^* apart on the rigid rotor internuclear axis, although d^* is not necessarily equal to the internuclear distance d. An attractive force is located on the molecular centre of mass. If A and B are the atoms in one molecule and C and D are the other, figure 1, the internuclear potential V is given by

$$V = \tfrac{1}{4}E^* \exp(\alpha D)[\exp(-\alpha R_{AC}) + \exp(-\alpha R_{AD}) + \exp(-\alpha R_{BC})$$
$$+ \exp(-\alpha R_{BD})] - 2E^* \exp[-\tfrac{1}{2}a(R - D)],$$

where R_{BC}, for example, is the distance between the atoms B and C. E^*, α and D are constants as described in Parker (1959).

The twelve equations of motion are derived from the Hamiltonian H expressed in terms of the momenta P

$$H = \frac{P_R^2}{2m} + \frac{P_\theta^2}{2mR^2} + \frac{P_\phi^2}{2mR\sin^2\theta} + \frac{P_{\beta_1}^2}{2I} + \frac{P_{\beta_1}^2}{2I} + \frac{P_{\psi_1}^2}{2I\sin^2\beta_1} + \frac{P_{\psi_2}^2}{2I\sin^2\beta_2}.$$

The calculations are performed in a frame of reference fixed in the centre of molecule 1 which has angular momentum J_1 and initial orientation defined by the angles ψ, and β_1, figure 1.
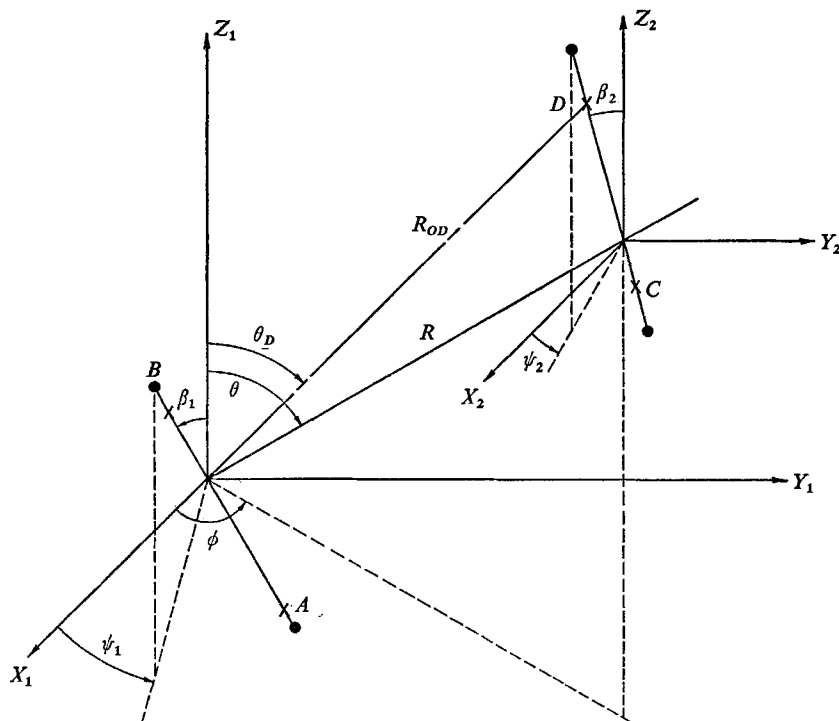

FIGURE 1. Co-ordinate system for collision model (from Lordi & Mates 1970).

Details of calculations

As full three-dimensional calculations require considerable computer time, the two-dimensional approximation which appeared to yield good results for Parker (1959) was used for some of the calculations. This effectively reduces the above equations to seven $\beta_i = \frac{1}{2}\pi$, $\theta = \frac{1}{2}\pi$, $P_\theta = 0$ and $P_{\beta_i} = 0$, i.e. the molecules only rotate in the collision plane. For these calculations 2000 particles were used and divided into 50 cells of initial width $1\cdot5\lambda$. Before the Monte Carlo scheme could be entered it was necessary to calculate the collision cross-sections for various collisional velocities g, rotational velocities and impact parameters b, figure 2. A typical collision trajectory is shown in the figure 2. The variation of the deflexion angle χ, (defined in figure 2) with impact parameter b for a range of relative collisional velocities is shown in figure 3. Generally the curves have been calculated for initial angular momenta $\hat{J}_1 = \hat{J}_2 = 1\cdot0$ as it was found that except for very low values of g no variation in χ is detectable with $\hat{J}$. With increasing collisional velocities the collision cross-section, here defined as the cross-section calculated with the value of b when $\chi < |0\cdot1°|$, tends to become constant. A negative value of χ represents a condition where the colliding molecule passes
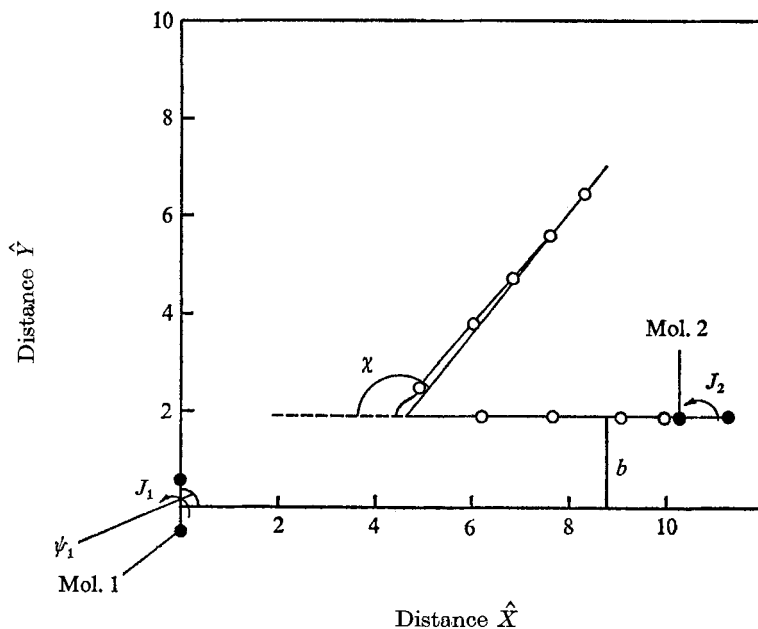
FIGURE 2. Typical collision trajectory. Both molecules have same initial spin $\hat{J}_1 = \hat{J}_2 = 1\cdot 0$ and are situated initially at right angles ($\psi_1 = \frac{1}{2}\pi$, $\psi_2 = 0$). Quantities indicated with (^) are non-dimensional; Lordi & Mates (1970).
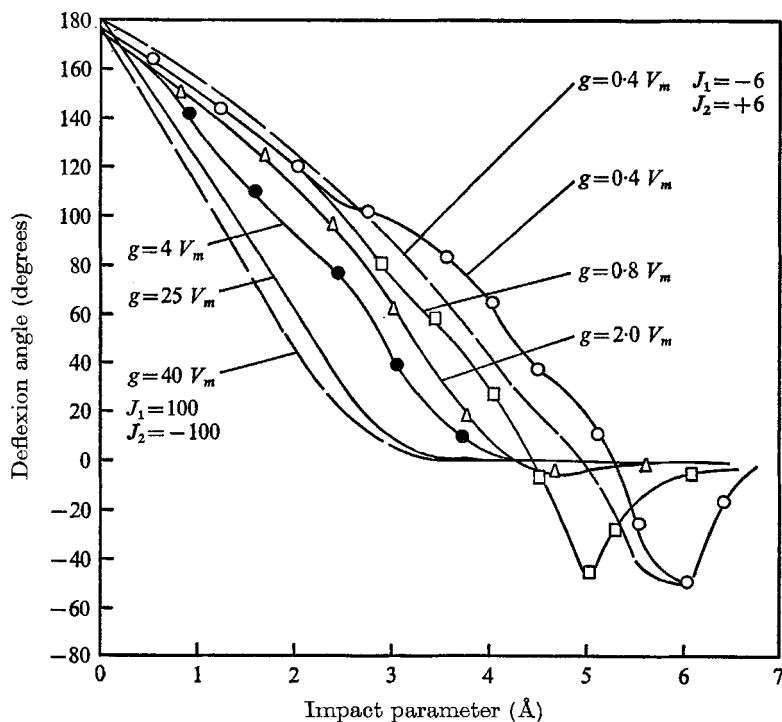

FIGURE 3. Variation of deflexion angle (χ) with impact parameter for colliding oxygen molecules with various collisional velocities (g). Except as noted both molecules initially with average rotational momenta ($\hat{J}_1 = \hat{J}_2 = 1\cdot 0$) with $\psi_1 = \frac{1}{2}\pi$, $\psi_2 = 0$. (See figure 1.)

behind the molecule fixed at the co-ordinate centre and the value of b, figure 2, becomes negative. The calculation was always started with $\hat{R} = 15$ and a value of $\hat{b}$ was chosen proportional to b, i.e. a greater probability of a glancing collision occurring than a central impact. The initial value of ψ_i is then chosen at random for each particle and the calculation commenced. The time increment was adjusted throughout the calculation to keep the total weighted error (Ralston 1960, p. 110), less than 10^{-4}. The collision was terminated when $\hat{R}$ again became greater than 15.

Additional problems arise in the three-dimensional calculations. Singularities occur in some of the derivatives as θ, β_i, ϕ, and ψ_i pass through various multiples of $\frac{1}{2}\pi$. In the present solution, if the angle was $1.5°$ from the singularity the derivative was calculated with the angle taken at $1.5°$ from the singularity. Provided the allowable weighted error was not too small this allowed the calculation to proceed satisfactorily. Again, with twelve equations to solve, the round-off error became greater and it was necessary to reduce the size of the allowable weighted error. Thus it was chosen as 10^{-2} for both the above reasons. In order to minimize the required computer time a system of 800 particles divided into 50 cells was used, although this reduced the accuracy obtained in the velocity frequency distribution. Again, the author should be contacted for a detailed description.

Results

Using the two-dimensional rotation assumption results were calculated for Mach numbers 7·0 and 12·9 as these were the Mach numbers at which Robben & Talbot (1966b) obtained results. The profiles of translational temperature, rotational temperature and density are shown in figure 4. When interpreting this and related figures, the actual plotted points should be examined as the curves are inserted for convenience only. The points used in drawing the pressure profiles are not shown in order to simplify the diagram. The pressure points may be obtained from the density and temperature points. As can be seen from figure 4, the post shock translational temperature is above the expected Rankine–Hugoniot value, the post shock density is below the expected value but the pressure and rotational temperature are as expected. The translational temperature of the gas appears to require a value of $\gamma \simeq 1.5$ and this may seem reasonable as only one degree of freedom was allowed for rotation. However it would appear that as the rotational temperature has achieved its expected value and the translational temperature is still too high an excess of energy has occurred. As will be discussed below this is not so and energy is in fact conserved. It was found possible to make the gas appear as a $\gamma \simeq 1.5$ gas by increasing the value of d^* from the value of 0.557 Å chosen by Parker (1959) to $d^* = 0.63$ Å. Under these conditions, the curves can be plotted to give apparently consistent results between both temperatures, density and pressure. In fact by increasing d^* still further the rotational temperature can be made to exceed the translational. A temperature overshoot at the top of the shock appears to occur in Mach number 7·0 results and as two points supported this for Mach 12·9, an overshoot is shown there too.
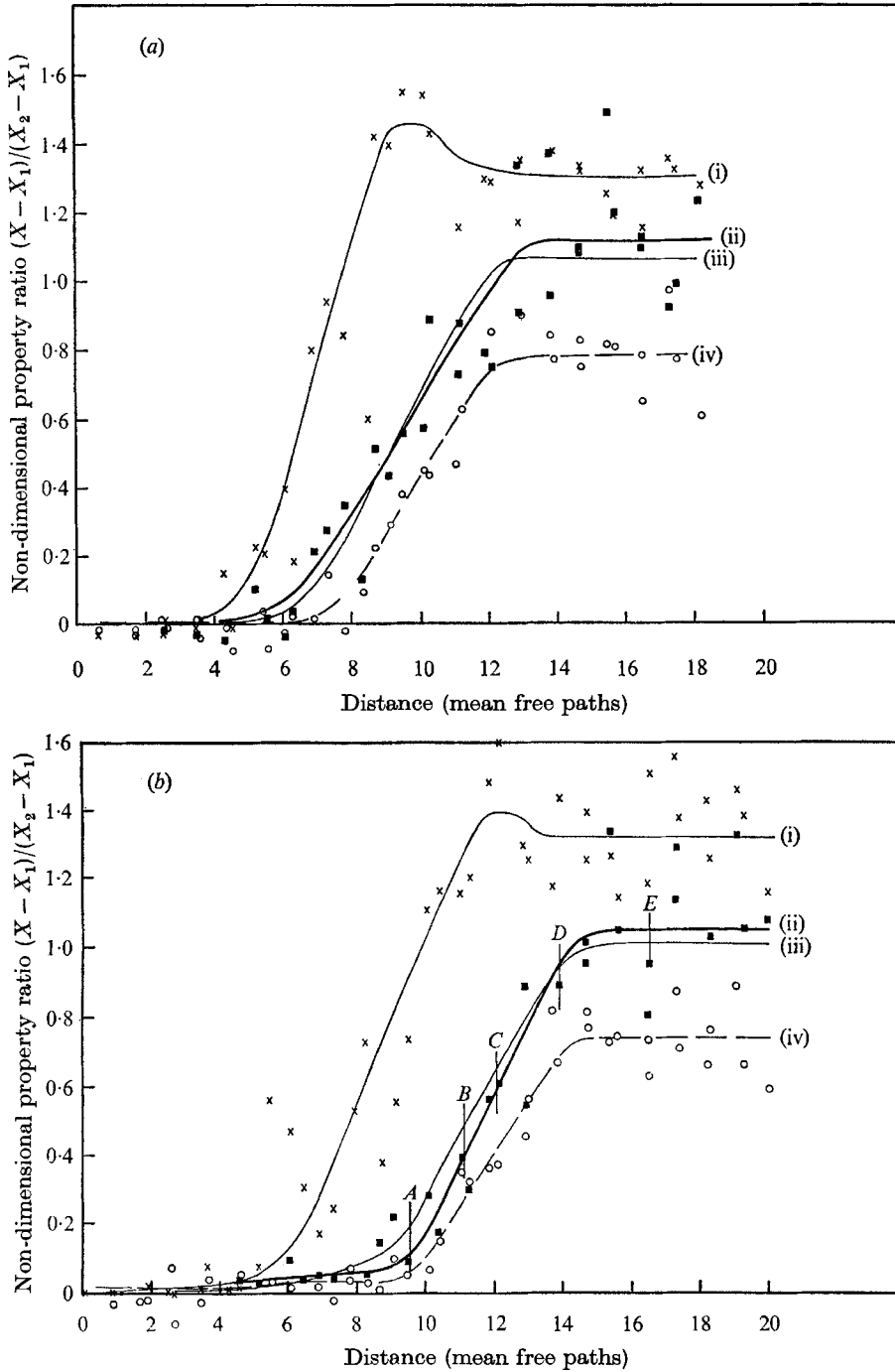
FIGURE 4. Variation of translational temperature, density and rotational temperature through shock waves in nitrogen, using two-dimensional simplification for rotational effects. Pressure variation is obtained from density and temperature curves. (a) Mach number 7·0, (b) Mach number 12·9. (i) Temperature (×), (ii) rotational temperature (■), (iii) pressure, (iv) density (○).

Although the Mach number is doubled from figure 4 (b) to figure 4 (a) there is virtually no difference between the rotational temperature profiles and the density profiles. This could mean that a maximum spacing has been reached by Mach number 10 or it could be an error due to the two-dimensional assumption. This question is not resolved in the present work.
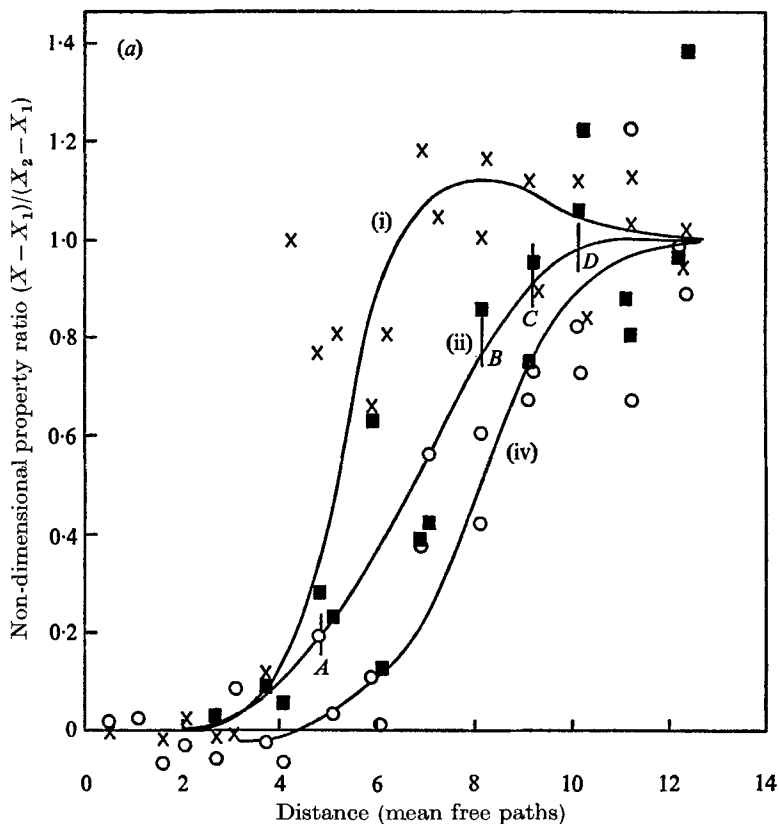

FIGURE 5. For legend see facing page.

A three-dimensional calculation was performed to examine the accuracy of the two-dimensional results. Initial running of the program quickly showed that the rotational relaxation time was very long when $d^* = 0.557$ Å. For example, by the time the post shock density value was achieved the rotational temperature was only about 50 % of the equilibrium value. This was also found by Lordi & Mates (1970) and it was pointed out there that d^* has been chosen by Parker matching his two-dimensional calculations to experiment. It was also stated that the two-dimensional approximation was the easy energy transfer case. Thus a large value of d^* closer to d, the internuclear distance, would be expected to apply to the three-dimensional calculations. The value of d was 1.094 Å (Parker 1959), so in the present calculations d^* was rather arbitrarily set as 0.9 Å. This figure was selected, as a similar calculation for oxygen, using a value of $d^* = 0.91d$ appeared to be possibly too high. Thus the value of d^* here is $0.82d$. A shock wave of Mach number 11.2 was generated as only one result could be obtained due to

the expense of the calculations. This appeared to lie about the middle of the available results due to Robben & Talbot (1966*b*) and Marrone (1967). The profiles of translational temperature, rotational temperature and density are shown in figure 5(*a*). The scatter in results is greater than for the two-dimensional calculations as less particles are used for these calculations. An overshoot is
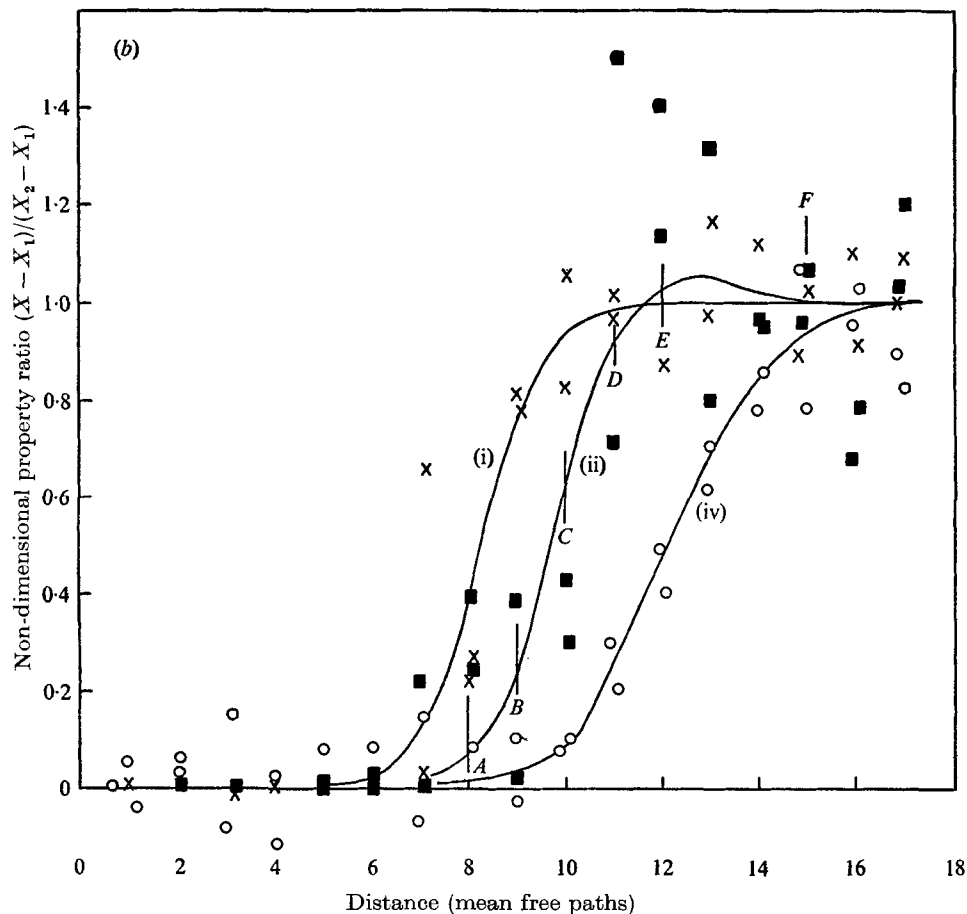

FIGURE 5. Variation of temperature, density and rotational temperature through shock waves using three-dimensional calculations. (*a*) Mach number 11·2 in nitrogen, (*b*) Mach number 17·8 in oxygen. See figure 4 for symbols.

apparently found at the top of the shock wave in the translational temperature profile. The most striking feature in comparing the two-dimensional and three-dimensional results is that the shock waves are thinner in the three-dimensional case. The two- and three-dimensional density and rotational temperature profiles can be made to coincide if the mean free path in the two-dimensional calculations is halved. This is due to there only being one degree of freedom in rotation, which does not require as much energy to be extracted from translational energy. Thus the density rises more slowly and a greater number of collisions is required. The translational temperature profiles can be made to coincide by altering the mean

free path in the two-dimensional calculation by about $\frac{2}{3}$. It was found in calculations for a shock wave of Mach number 17·8 in O_2, that a rotational temperature overshoot occurred, figure 5(b). The overshoot is probably due to selecting too large a value for d^*. If the three high points are ignored, figure 5(b), a profile similar to the nitrogen profile is obtained for rotational temperature. Thus it appears that the two-dimensional calculations can be used to predict the three-dimensional behaviour.

An examination of the rotational velocity frequency distributions for both the two-dimensional and three-dimensional cases are shown in figure 6(a) and (b). The letter references on the curves refer to the appropriate positions on the shock profile in figures 4(b) and 5(a) respectively. The curves at station A have been rather arbitrarily rounded at the peak values as few particles are contained in the cells in this part of the shock wave. It was found that the initial distribution is similar in both two-dimensional and three-dimensional calculations. About half way up the shock profile a bi-modal structure is obtained in both calculations, however the mean of the second Maxwellians do not coincide in the two-dimensional and three-dimensional calculations. The existence of a bi-modal form at this point is in agreement with the experimental work of both Robben & Talbot (1966b) and Marrone (1967). The present results suggest that a Maxwellian is formed in the three-dimensional results before the top of the shock wave is reached. In results using oxygen, it was found that the bi-modal form persisted to the top of the shock wave. However, the two-dimensional results show that an almost uniform frequency of velocities is obtained in the post shock region. The cause of the two-dimensional calculations indicating an incorrect frequency distribution can be seen if the impact parameter at the point of closest approach is thought to have two orthogonal components b_1, b_2 in the three-dimensional calculations. In the two-dimensional calculations b_2, say, is always 0, thus if b is chosen proportional to b in both the two- and three-dimensional calculations, the average value of b at the point of closest approach will be smaller in the two-dimensional than the three-dimensional case. This may be overcome by choosing b proportional to b^2 for the two-dimensional calculations. However, the relaxation distance would be larger and a larger value of d^* probably would be necessary. An examination of the translational velocity distribution gave approximately Maxwellian distributions in both cases. Due to the number of points available, the curves were not sufficiently defined to be certain that both were identical. From a visual examination it did appear to be so although there are theoretical reasons to doubt that if the rotational velocity is non-Maxwellian then the translational temperature could be strictly Maxwellian. Generally it appears that the result of the two-dimensional calculations must be viewed with great care.

Another physical quantity that can be obtained from the Monte Carlo calculations is the number of collisions the average particle will undergo in passing through the shock wave. The results for both nitrogen and oxygen are shown in figures 7(a) and 7(b) and the curves of temperature and density are superimposed from figures 6(a) and 6(b) respectively. The number of collisions are measured from the cell where the first high speed particle was found, i.e. $V/V_m > 8$. It was found by Talbot & Scala (1961) that 5 collisions were required for rotational
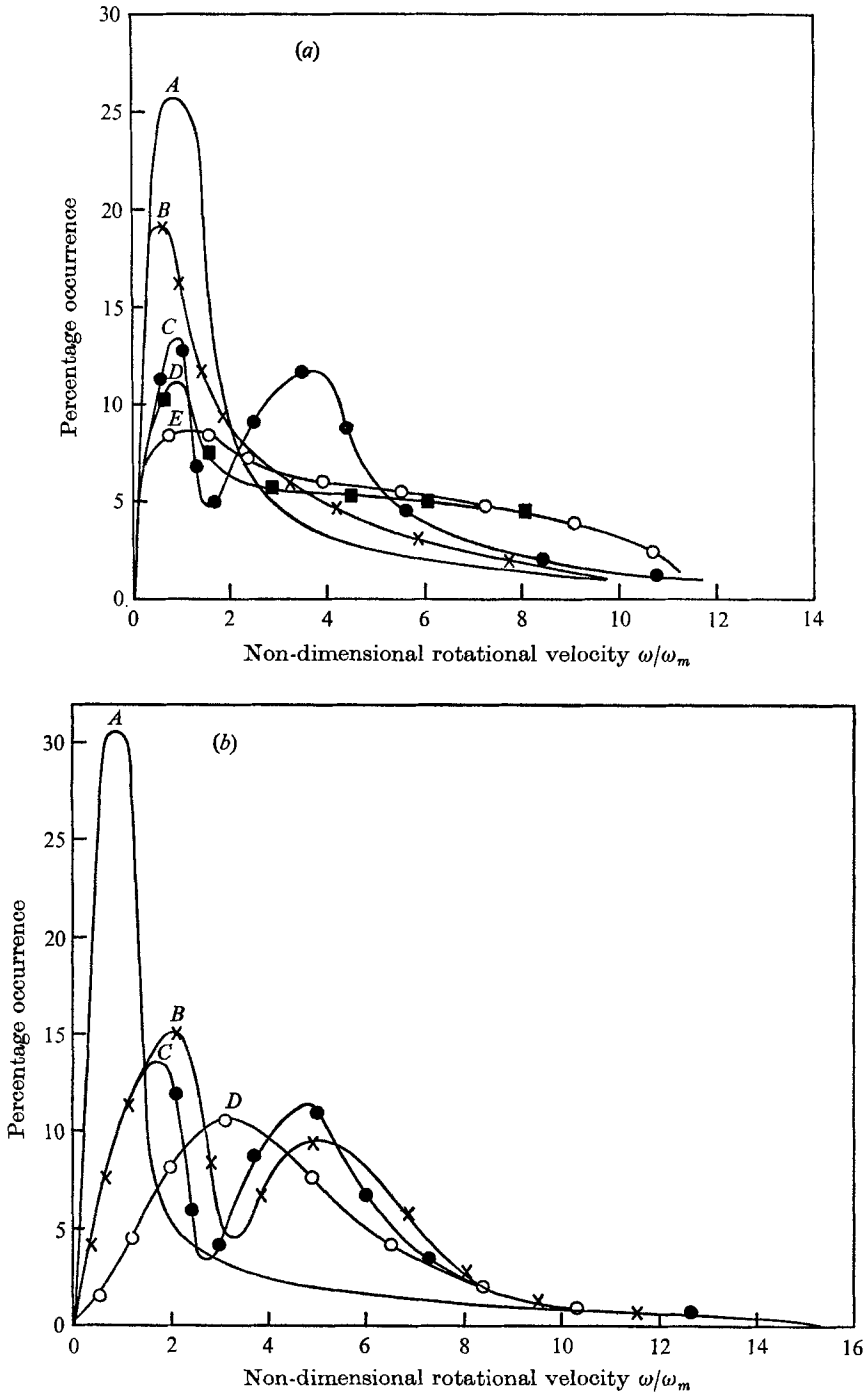
FIGURE 6. Frequency distribution of rotational velocity through shock waves at various stations. (a) Mach number 12·9, two-dimensional calculations, (b) Mach number 11·2, three-dimensional calculations.
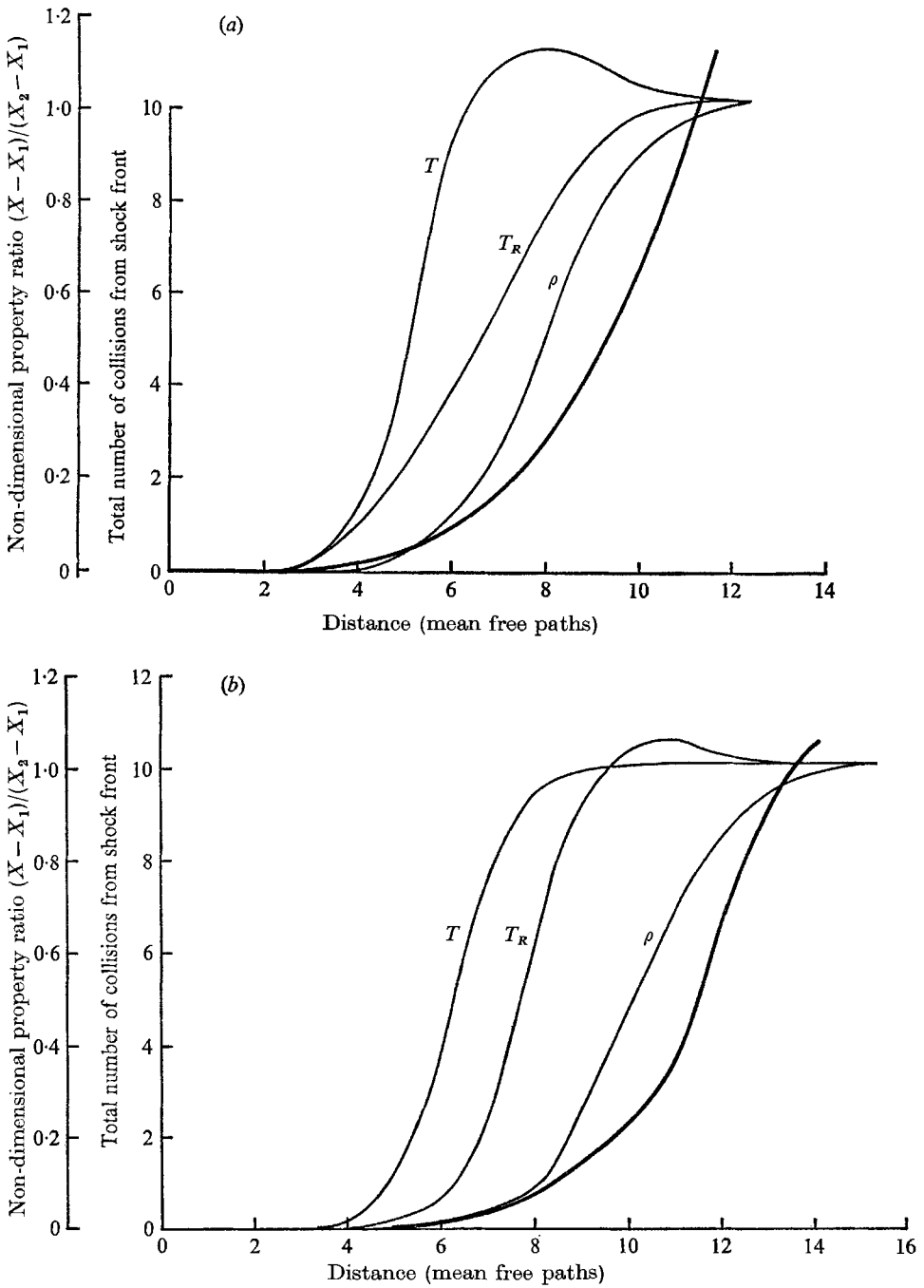
FIGURE 7. Number of collisions average molecule will experience in passing through shock waves plotted as function of distance through shock wave. (a) Nitrogen gas Mach number 11·2, (b) oxygen gas Mach number 17·8.

relaxation. It can be seen that the nitrogen results agree with this but that the oxygen results give a figure of $Z_R = 3$. If the overshoot region in the oxygen results is ignored, that is, the three high temperature points, $Z_R = 5$. This again could suggest that d^* was chosen as too large a fraction of d, i.e. insufficient allowance was made for the effect of electron cloud distortion due to forming the molecule. On the other hand the result may be correct. It was found by Robben &
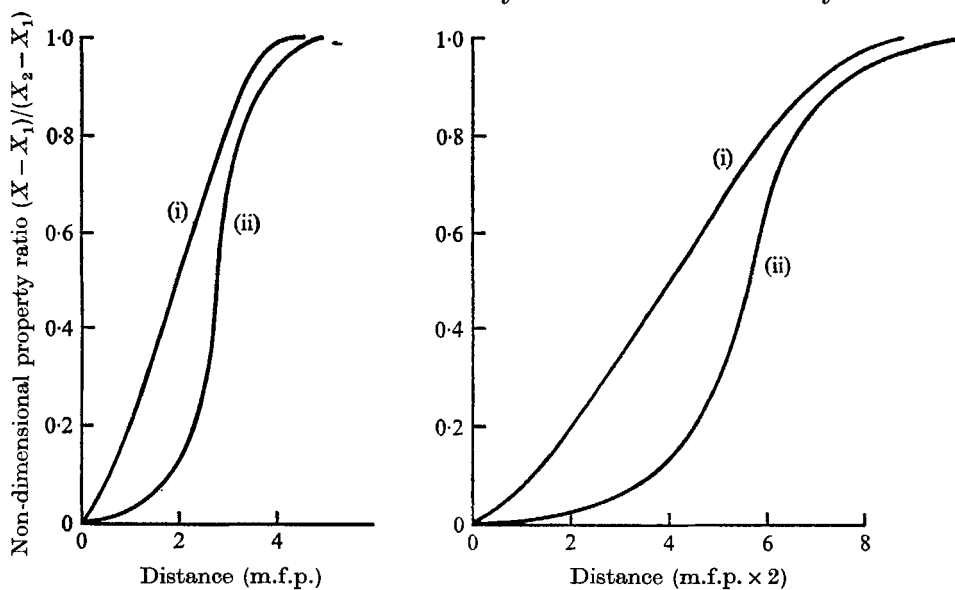

FIGURE 8. Normalized density and rotational temperature profiles for a Mach number 12·9 shock wave in nitrogen from Robben & Talbot (1966b). Abscissa: (a) mean free path as estimated from original results; (b) twice mean free path. (i) rotational temperature; (ii) density.

Talbot (1966b) that as the Mach number increases the rotational temperature profile moved ahead of the density profile. Thus as the nitrogen results are for Mach number 11·2 and the oxygen is at 17·8, the difference may be due to the Mach number difference only. Experimental results at this Mach number would settle the question. It seems rather futile to attempt to estimate the required number of collisions to closer than the nearest integer. It may be seen that translational temperature equilibrium is obtained in about one collision. Density equilibrium requires at least twelve collisions for nitrogen and fourteen for oxygen.

To compare the present results with experiment, it is necessary to estimate the upstream mean free path in the experiments by Robben & Talbot (1966b). As the stagnation pressures were not given for the experiments conducted at Mach number 12·9, the calibration results (Robben & Talbot 1966a) were used to estimate the value of P_0 in Robben & Talbot (1966b) as 160 torr. This was then combined with the collision cross-section calculated from $b = 4.25$ Å, which was used to estimate λ in the present work. As the cross-section is a function of rotational velocity in the low collisional velocity régime, the calculation of the mean free path would involve a fairly detailed calculation over all velocity

régimes. Further it is not at all clear whether the collision cross-section for the mean free path should include the negative values of χ. As the same value was to be used in the calculated and experimental results, it was not important for the comparison whether the exactly correct value of b was used. Figure 8(a) shows the shock-wave profiles for density and rotational temperature from Robben & Talbot (1966b) plotted on the present mean free path scale. It can be seen that the shock-wave thicknesses are much less than the present calculations shown in figure 5(a). In fact, if the mean free path is doubled, figure 8(b), curves very close to those in figure 5(a) are obtained. This discrepency was noted although not explained by Robben & Talbot (1966b) when they compared their results with those by Camac (1966). Similarly Marrone (1967) found that the shock-wave thickness calculated from his experiments were approximately twice those by Robben & Talbot (1966b). Thus it would appear that the present results would compare well with the results by Marrone and that the general relationship between the rate of rise of rotational temperature and density is similar to those by Robben & Talbot (1966b) except for the difference in length scale.

An examination of the variation of the bi-modal frequency distribution measured by Robbon & Talbot (1966b) shows that the original Maxwellian has disappeared by 8 mean free paths from the shock front using the modified length scale. This is before the equilibrium condition has been achieved and compares with 10 in the pressure results found with the Monte Carlo method for nitrogen. As this did not occur with the oxygen results, it suggests again that d^* for oxygen was taken as too great a fraction of the internuclear distance. The results of Robben & Talbot (1966b) show the strongest bimodal structure at about 3 mean free paths from the shock foot whereas the present results suggest 7 mean free paths. It must be considered, however, that the experimental results have been obtained using an equilibrium theory to deduce the distribution frequency. This could contain some error. This again shows that a comparison of the frequency distributions between theory and experiment is crucial.

It would be possible to use the frequency distribution curves to study the way the two Maxwellian distributions interact with each other through the shock wave. Thus values of $n_1(x)$ and $n_2(x)$, the number density in each Maxwellian, could be found. This has not been undertaken as the curves in figure 6(b) are only obtained from between 15 and 75 particles depending on the cell. It was not felt that the results were sufficiently accurate to justify any quantitative calculations. The curves in figure 7(b) are only sufficient to demonstrate the difference between the two- and three-dimensional calculations. More extensive results would be necessary to define the curves accurately enough for quantitative results of $n_1(x)$ and $n_2(x)$ to be obtained. Before such an exercise is worthwhile the intermolecular potential must be obtained with greater accuracy. Possibly the study of gaseous hydrogen would provide a more meaningful calculation.

Conclusion

The relationships between the rotational temperature profiles, density and translational temperature profiles through shock waves in nitrogen have been

calculated and compared with experimental results. It was found that the comparison was good provided the experimental results were altered to compare with other works in the field, i.e. that the shock-wave thickness should be increased. Rotational collision numbers Z_R were calculated for both oxygen and nitrogen and a value of 5 was found probably true for both. The oxygen results were in some doubt as the spacing between the molecular repulsive centres was possibly chosen to be too large. The actual calculated results for oxygen gave a rotational temperature overshoot $Z_R = 3$. As a good comparison between experiment and theory has been found for nitrogen with d^*, the distance between repulsive centres, equal to 0·82 the internuclei distance, this would seem approximately the correct fraction. Some calculations were also performed using a two-dimensional approximation in common use. It was found that although the right temperature and density profiles could be obtained, the rotational frequency distribution was non-Maxwellian downstream. It is suggested this may be corrected by choosing different values of d^* and the probability relationship for impact parameter selection. The eventual refinement of such calculations as these depend upon a better knowledge of internuclear potential functions.

REFERENCES

CAMAC, M. 1966 *Rarefied Gas Dynamics* (ed. J. H. de Leeuw). New York: Academic.

CURTISS, C. F. 1956 *J. Chem. Phys.* **24**, 225.

DENISIK, S. A., MALAMA, YU. G., POLAK, L. S. & REZANOV, R. A. 1967 *Teplofizika Vysolikh Temperatur,* **5**, 1011.

LORDI, J. A. & MATES, R. E. 1970 *Phys. Fluids,* **13**, 291.

MACPHERSON, A. K. 1969 *J. Fluid Mech.* **39**, 849.

MARRONE, P. V. 1967 *Phys. Fluids,* **5**, 80.

MUNTZ, E. P. 1962 *Phys. Fluids,* **5**, 80.

PARKER, J. G. 1959 *Phys. Fluids,* **2**, 449.

RALSTON, W. 1960 *Mathematical Methods for Digital Computers.* New York: Wiley.

ROBBEN, F. & TALBOT, L. 1966*a Phys. Fluids,* **9**, 633.

ROBBEN, F. & TALBOT, L. 1966*b Phys. Fluids,* **9**, 653.

TALBOT, L. & SCALA, S. C. 1961 *Rarefield Gas Dynamics* (ed. L. Talbot). New York: Academic.

TAXMAN, N. 1958 *Phys. Rev.* **110**, 1235.

WANG CHANG, C. S., UHLENBECK, G. E. & DE BOER 1964 *Studies in Statistical Mechanics.* Amsterdam: North-Holland.

WANG CHANG, C. S., UHLENBECK, G. E. & TAXMAN, N. 1961 *Michigan University Engineering Research Institute Rep.* no. cm-681.